

# Calculation of the axial charge in the $\epsilon$ and $\epsilon'$ regimes of HBChPT

Brian Smigielski\* and Joseph Wasem†  
*Department of Physics, University of Washington*  
*Box 351560, Seattle, WA 98195, USA*  
 (Dated: June 26, 2007)

The axial charge  $g_A$  is calculated in the  $\epsilon$  regime of Heavy Baryon Chiral Perturbation Theory to order  $\epsilon^3$ . To perform this calculation, we develop a technique to compute baryon properties in the  $\epsilon$  regime of Chiral Perturbation Theory. This technique includes contributions from pion zero momentum modes and can be used at arbitrary order, diagram by diagram, in the  $\epsilon$  regime to calculate any matrix element. Also, a calculation of  $g_A$  in the  $\epsilon'$  regime to order  $\epsilon'^3$  is performed. A discussion of the domain of applicability for both the  $\epsilon$  and  $\epsilon'$  regimes is also included.

## I. INTRODUCTION

As computational speed has steadily advanced in recent years, lattice QCD has been increasingly utilized as the only known method of computing observables directly from QCD. However, even the most advanced calculations to date use moderate lattice volumes and unphysically large pion masses. State of the art calculations are performed with the spatial length of the lattice being on the order of a few Fermis, while the temporal extent is typically larger by at most a factor of three. These calculations are also done with pion masses that are at least a factor of two greater than the physical pion mass. In studying low energy observables using lattice QCD it is therefore important to fully understand how the finite volume of the lattice and the large pion mass affect the result. To study the low energy dynamics of QCD and finite volume effects thereof Chiral Perturbation Theory (ChPT) in finite volume can be used.

When studying baryon properties the low energy theory used is Heavy Baryon Chiral Perturbation Theory (HBChPT)[1]. For infinite volume HBChPT, the small expansion parameters are  $\Lambda_{\text{QCD}}/m_B$ ,  $p/\Lambda_\chi$ , and  $m_\pi/\Lambda_\chi$  where  $p$  is the typical momentum and  $\Lambda_\chi$  is the chiral symmetry breaking scale typically of order 1 GeV[2]. This counting scheme also holds in finite volume when  $m_\pi L/2\pi \gg 1$ . However, a problem exists for small quark masses ( $m_\pi L/2\pi \ll 1$ ), as the zero momentum mode pion propagator goes as  $1/m_\pi^2 V$ , where  $V$  is the spacetime volume[3]. Thus as computational power continues to increase and lattice calculations are performed at ever lower quark masses, the contribution from zero momentum mode pions will become ever larger. To account for this in the HBChPT calculation the counting scheme must be changed to enhance the order at which zero mode diagrams contribute.

To remedy this problem, the construction of a new power counting scheme is needed such that the zero momentum modes are enhanced and integrated over exactly while the non-zero momentum modes can be treated perturbatively[3, 4, 5, 6, 7, 8, 9]. This leads to the formulation of the  $\epsilon$  regime. In the  $\epsilon$  regime, if  $L$  and  $\beta$  are, respectively, the spatial and temporal extent of the box one is working in,  $\epsilon \sim 2\pi/\Lambda_\chi L \sim 2\pi/\Lambda_\chi \beta$  and  $\epsilon^2 \sim m_\pi/\Lambda_\chi$ . This counting takes

---

\*Electronic address: smigs@u.washington.edu

†Electronic address: wasem@u.washington.edu

into account that the zero momentum pion contributions have become nonperturbative. The integration over these zero modes is achieved by utilizing the method of collective variables[3] and methods for including baryons in this framework have been proposed previously[10].

Another important regime for working in small volumes in is the  $\epsilon'$  regime[11]. This regime is characterized by a highly asymmetric hyperbox with spatial dimension  $L$  and a large temporal dimension. Due to the zero mode pion propagator mentioned above (which goes as  $1/m_\pi^2 V$ ), as one approaches the  $\epsilon$  regime from the  $p$  regime the spatial and temporal zero modes will become enhanced relative to the nonzero modes. While they do not yet need to be treated nonperturbatively, their counting does need to be enhanced relative to the nonzero modes. To account for this, the  $\epsilon'$  regime possesses similar counting rules to the  $\epsilon$  regime:  $\epsilon' \sim 2\pi/\Lambda_\chi L$  and  $\epsilon'^2 \sim m_\pi/\Lambda_\chi$ , but separate rules for the temporal counting. For nonzero momentum modes the time direction counts according to  $\epsilon' \sim 2\pi/\Lambda_\chi \beta$ . However, for pion loops containing spatial zero modes this counting changes to  $\epsilon'^2 \sim 2\pi/\Lambda_\chi \beta$ . In this regime, zero modes remain perturbative. For the specific combinations of the lattice size and quark mass used in this paper, the  $\epsilon$  and  $\epsilon'$  regimes are the correct counting schemes to use.

The axial-vector current has been previously studied in the  $p$  regime in finite volume[12] and provides an important cornerstone of lattice QCD efforts to understand baryon physics[14, 15, 16, 17, 18, 19]. This work focuses on understanding the nonperturbative aspects of the  $\epsilon$  regime and computing the axial-vector current matrix element between two nucleon states of equal momenta for lattice sizes that require the use of the  $\epsilon$  and  $\epsilon'$  regimes of HBChPT. By better understanding how the volume of the lattice and choice of quark mass determines which power counting scheme is needed, one can more accurately extrapolate the infinite volume, physical pion mass results for  $g_A$  from the lattice data.

## II. HEAVY BARYON CHIRAL PERTURBATION THEORY

At low energy one can use HBChPT to describe the dynamics of nucleons and pions. The Lagrangian that is consistent with spontaneously broken  $SU(2)_L \otimes SU(2)_R$  is at leading order[1, 20]:

$$\begin{aligned}
\mathcal{L}_0 = & \bar{N} i v \cdot \mathcal{D} N - \bar{T}_\mu i v \cdot \mathcal{D} T^\mu + \Delta \bar{T}_\mu T^\mu + \frac{f^2}{8} \text{Tr}[\partial_\mu \Sigma^\dagger \partial^\mu \Sigma] \\
& + \lambda \frac{f^2}{4} \text{Tr}[m_q \Sigma^\dagger + h.c.] + \lambda C_1 \bar{N} \text{Tr}[m_q \Sigma^\dagger + h.c.] N + 2g_A^{(0)} \bar{N} S^\mu \mathcal{A}_\mu N \\
& + g_{\Delta N} [\bar{T}^{abc,\nu} \mathcal{A}_{a,\nu}^d N_b \epsilon_{cd} + h.c.] + 2g_{\Delta\Delta} \bar{T}_\nu S^\mu \mathcal{A}_\mu T^\nu
\end{aligned} \tag{1}$$

with the velocity dependent nucleon fields  $N$  (for brevity in this paper the usual subscript  $v$  and the integral over the velocity have been dropped from the nucleon fields), the Rarita-Schwinger fields  $T^\mu$  describing the  $\Delta$ -resonances, and

the definitions:

$$\begin{aligned}
\Sigma &= \xi^2 = \exp\left(\frac{2iM}{f}\right), \\
M &= \begin{pmatrix} \pi^0/\sqrt{2} & \pi^+ \\ \pi^- & -\pi^0/\sqrt{2} \end{pmatrix}, \\
\mathcal{A}^\mu &= \frac{i}{2}(\xi\partial^\mu\xi^\dagger - \xi^\dagger\partial^\mu\xi), \\
V^\mu &= \frac{1}{2}(\xi\partial^\mu\xi^\dagger + \xi^\dagger\partial^\mu\xi), \\
\mathcal{D}^\mu &= \partial^\mu + V^\mu.
\end{aligned} \tag{2}$$

The pion fields are encapsulated in the matrix  $M$ . The Rarita-Schwinger fields are rank-3 tensors such that:

$$T^{111} = \Delta^{++}, \quad T^{112} = \frac{1}{\sqrt{3}}\Delta^+, \quad T^{122} = \frac{1}{\sqrt{3}}\Delta^0, \quad T^{222} = \Delta^- \tag{3}$$

while the nucleons are simply an SU(2) vector given by

$$N = \begin{pmatrix} p \\ n \end{pmatrix} \tag{4}$$

where the constant  $f = 132$  MeV and the matrix  $m_q$  is the quark mass matrix. The three couplings given in eqn. (1) ( $g_A^{(0)}$ ,  $g_{\Delta N}$ , and  $g_{\Delta\Delta}$ ) are the infinite volume, chiral limit couplings between baryons and pions. Also,  $S^\mu$  is the covariant spin vector and  $v^\mu$  is the heavy baryon four velocity with  $v^2 = 1$  (typically  $v^\mu = (1, \vec{0})$ ).

In our calculation higher order Lagrangian terms will also become important. The relevant next to leading order Lagrangian terms are:

$$\begin{aligned}
\mathcal{L}_1 &= -\left(\bar{N}\frac{\mathcal{D}^2 - (v \cdot \mathcal{D})^2}{2m_B}N\right) + \left(\bar{T}^\mu\frac{\mathcal{D}^2 - (v \cdot \mathcal{D})^2}{2m_B}T_\mu\right) + 4\bar{N}\left(C_2 - \frac{g_A^{(0)2}}{8m_B}\right)\mathcal{A}_0^2N + 4C_3\bar{N}\mathcal{A}^\mu\mathcal{A}_\mu N \\
&\longrightarrow \bar{N}\frac{\vec{\partial}^2}{2m_B}N - \bar{T}^\mu\frac{\vec{\partial}^2}{2m_B}T_\mu + 4\bar{N}\left(C_2 - \frac{g_A^{(0)2}}{8m_B}\right)\mathcal{A}_0^2N + 4C_3\bar{N}\mathcal{A}^\mu\mathcal{A}_\mu N
\end{aligned} \tag{5}$$

where the chirally covariant derivatives  $\mathcal{D}$  are converted to normal derivatives  $\partial$  as the contributions from  $V^\mu$  will not be important at the order considered. The coefficients in front of these terms are determined by reparametrization invariance[21]. The last two terms are not be important for calculating the axial matrix element to order  $\epsilon^3$  or  $\epsilon'^3$ , but are important for the nucleon mass. The first two terms in eqn. (5) are simple higher order extensions of the kinetic energy operators given in the lowest order Lagrangian. Including these terms modifies our baryon and decuplet propagators. It should also be noted that these two order  $1/m_B$  terms are not the only  $1/m_B$  operators, but they are the only ones that will enter in the evaluation of the axial matrix element to the order we work in  $\epsilon$  and  $\epsilon'$ . Defining  $\tau_{\xi_+}^a = \frac{1}{2}(\xi^\dagger\tau^a\xi + \xi\tau^a\xi^\dagger)$  and  $\tau_{\xi_-}^a = \frac{1}{2}(\xi^\dagger\tau^a\xi - \xi\tau^a\xi^\dagger)$ , the axial-vector current is:

$$j_{\mu 5}^a = g_A^{(0)}\bar{N}S^\mu\tau_{\xi_+}^aN + \frac{1}{2}g_{\Delta N}\left(\bar{T}^{abc,\mu}(\tau_{\xi_+}^a)_a^d N_b\epsilon_{cd} + h.c.\right) + g_{\Delta\Delta}\bar{T}S^\mu\tau_{\xi_+}^aT + \bar{N}v^\mu\tau_{\xi_-}^aN + \dots \tag{6}$$

where the ellipses indicate higher order terms. The form of the higher order current is easily derivable by beginning with the fully relativistic expression for the current, and then substituting in the appropriate expansion for the

relativistic field in terms of the heavy field to the desired order in  $1/m_B$ . Upon doing this, and working to  $\mathcal{O}(\frac{1}{m_B})$ , the higher order current is[22, 23]:

$$j_{\mu 5}^{a,(1)} = \bar{N} \Gamma_{\mu}^a \left( \frac{i \vec{\mathcal{D}}_{\perp}}{2m_B} \right) N - \bar{N} \left( \frac{i \overleftarrow{\mathcal{D}}_{\perp}}{2m_B} \right) \Gamma_{\mu}^a N \quad (7)$$

where  $\mathcal{D}_{\perp} = \mathcal{D} - \not{v} (v \cdot D)$ ,  $\Gamma_{\mu}^a = S_{\mu} \tau_{\xi_{\perp}}^a$ , and the superscript (1) denotes  $1/m_B$  suppressed contribution to the current. Working to lowest order in the above current amounts to the replacement of  $\mathcal{D}$  by  $\not{\partial}$ . At tree level, this contribution vanishes as it is proportional to the spatial on-shell momenta which is taken to zero at the end. Similarly, including this operator within a loop diagram yields zero. This can be understood simply since both the pion propagator and the two pion-baryon vertices are even with respect to the spatial loop momenta whereas the higher order current supplies an odd power of the spatial loop momenta. These higher order terms will not be necessary for this calculation.

In finite volume, the fully relativistic nucleon field must satisfy the conditions[10]:

$$\begin{aligned} \psi(t, \vec{r} + \vec{n}L) &= -\psi(t, \vec{r}), \\ \psi(\beta, \vec{r}) &= -\psi(0, \vec{r}) \end{aligned} \quad (8)$$

where  $\beta$  is the temporal extent of the volume. Choosing the rest frame of the nucleon  $v^{\mu} = (1, 0, 0, 0)$ , this then implies that the heavy nucleon field satisfies the condition:

$$N(\beta, \vec{r}) = -e^{\beta m_B} N(0, \vec{r}). \quad (9)$$

This means that the heavy nucleon field has the Fourier decomposition

$$N(\tau, \vec{r}) = \sum_{n_0} \exp \left[ -i \left( \frac{\pi(2n_0 + 1)}{\beta} + im_B \right) \tau \right] N(0, \vec{r}). \quad (10)$$

A similar condition exists for the decuplet fields. The presence of the baryon mass in the above equation will become important when looking at the finite time corrections to Feynman graphs.

### III. $\epsilon$ AND $\epsilon'$ EXPANSION REGIMES OF VALIDITY

For a nucleon in a finite volume there are four different regimes that are dependent on the choices of the quark mass (and by extension the pion mass), the spatial extent of the volume, and the temporal extent of the volume. These regimes define particular power countings appropriate for the physics and are variously called  $\epsilon$ ,  $\delta$ , and  $\epsilon'$ [2, 3, 11, 24]regimes, along with the standard  $p$  regime. A simple illustration of the boundaries between them can be provided by examining how the different modes contained in the simple pion loop in fig. (1) count. This definition of the boundaries is not unique but serves as a useful guide. Concentrating on the  $\epsilon$ ,  $\delta$ , and  $\epsilon'$  regimes, each of these three expansion parameters are similarly defined by the relation:

$$\epsilon \sim \epsilon' \sim \delta \sim \frac{2\pi}{\Lambda_{\chi} L}. \quad (11)$$

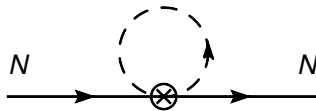


FIG. 1: One Loop Contribution

A useful relation to separate these regimes from the  $p$  regime is the condition

$$\frac{m_\pi L}{2\pi} < 1 \quad (12)$$

which is a quantity that counts as  $\epsilon$  or  $\epsilon'$ , and allows for a perturbative expansion in  $m_\pi L$ .

Examining the different modes of fig. (1) yields:

$$I \sim \frac{1}{\beta L^3} \sum_{n_\mu} \frac{1}{q_0^2 + |\vec{q}|^2 + m_\pi^2} \sim \begin{bmatrix} \frac{1}{\beta L^3 m_\pi^2}, & q_\mu = (0, \vec{0}) \\ \frac{\beta}{L^3}, & q_\mu = (q_0, \vec{0}) \\ \frac{1}{\beta L}, & q_\mu = (q_0, \vec{q}) \end{bmatrix} \quad (13)$$

where in finite volume one has the definitions  $|\vec{q}|^2 = (2\pi)^2(n_1^2 + n_2^2 + n_3^2)/L^2$  and  $q_0^2 = (2\pi)^2 n_0^2/\beta^2$ . The spatial and temporal zero modes are then defined by  $\vec{n} = 0$  and  $n_0 = 0$  respectively. To separate the three regimes ( $\epsilon$ ,  $\delta$ , and  $\epsilon'$ ) one must look at the boundaries of where both the spatial and the temporal zero mode enter at order one.

Also of interest is the quantity  $\Delta L/2\pi$ . It should be noted that strictly speaking  $\Delta L \gg 1$  because  $\Delta \sim \Lambda_{\text{QCD}} \sim f_\pi$  and in order for hadronic physics to be contained within the volume we work,  $f_\pi L \gg 1$ . Calculationally however,  $\frac{\Delta L}{2\pi}$  is numerically the same as  $\frac{m_\pi L}{2\pi}$  in the region of the  $\epsilon$  and  $\epsilon'$  regimes that are of primary interest to lattice QCD calculations, and this allows for a perturbative expansion of  $\Delta L/2\pi$ .

In the  $\epsilon$  regime it is required that the zero mode  $q_\mu = (0, \vec{0})$  counts as order one, while the  $\delta$  regime also requires that the spatial zero modes  $q_\mu = (q_0, \vec{0})$  count as order one. In the  $\epsilon'$  regime all zero mode contributions are perturbative. Utilizing this information, the boundaries of the three regimes in  $L$ - $m_\pi$  space for different values of the ratio  $\beta/L$  are plotted in fig. (2). However, it must be emphasized that these boundaries are necessarily very poorly defined in their placement, and should be interpreted more as midpoints in the smooth transition between regimes than as hard lines demarcating each region.

Within each of the regimes, how the pion mass, the decuplet mass splitting, and zero mode  $\beta$  count will vary depending on how the ratios  $m_\pi/\Lambda_\chi$ ,  $\Delta/\Lambda_\chi$ , and  $2\pi/\Lambda_\chi\beta$  compare to the ratio  $2\pi/\Lambda_\chi L$ . This will in turn affect the order at which certain graphs contribute. In this work  $m_\pi/\Lambda_\chi \sim \epsilon^2 \sim \epsilon'^2$  and  $\Delta/\Lambda_\chi \sim \epsilon^2 \sim \epsilon'^2$ . However, it should be noted that as one moves toward lattices with smaller spatial dimension and smaller pion mass both  $m_\pi/\Lambda_\chi$  and  $\Delta/\Lambda_\chi$  will numerically become smaller relative to  $2\pi/\Lambda_\chi L$  and so will count at higher order. This will require a reassessment of the order at which the graphs contribute.

Additionally, the order at which  $m_\pi$  contributes will have nontrivial consequences for how  $1/\beta$  is counted within the  $\epsilon'$  regime. In this work the zero mode counting of  $1/\beta$  in the  $\epsilon'$  regime is determined by  $m_\pi$ , as this is where the

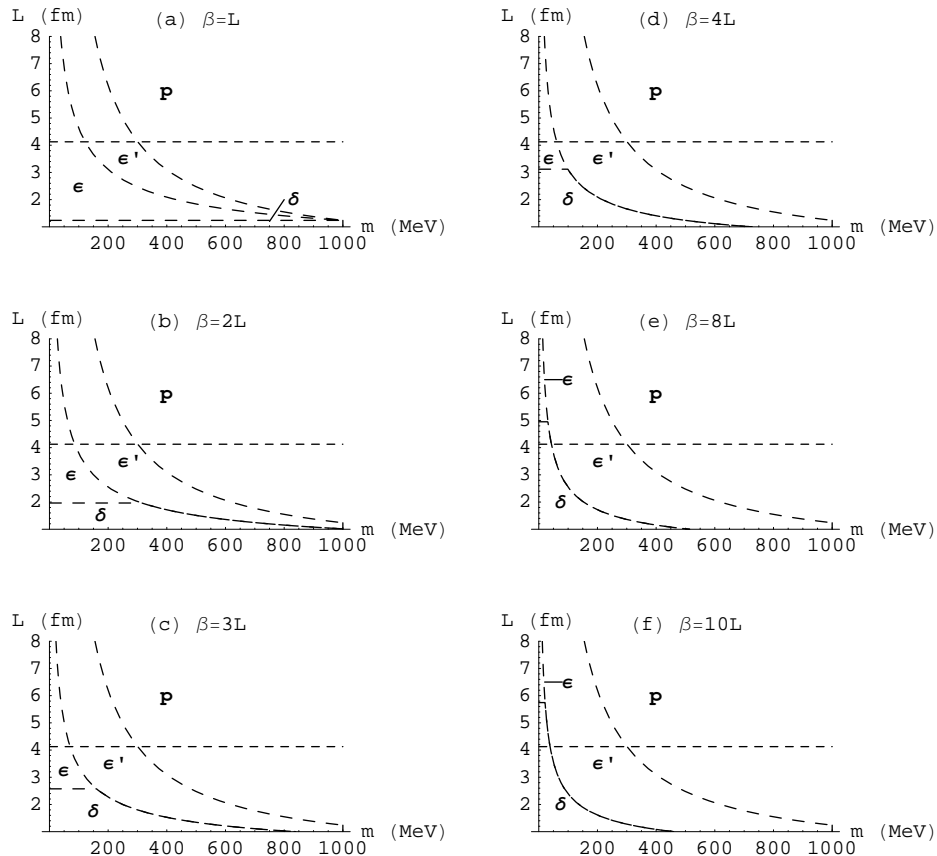


FIG. 2: Different counting regimes in  $L$ - $m_\pi$  space. The horizontal dashed line gives the value of  $2\pi/\Delta$  above which the expansion taken in  $\Delta L$  is no longer valid. The dashed lines demarcating the boundaries between the different regions are there to remind the reader that these are poorly defined boundaries.

zero mode of the tadpole diagram of fig. (1) becomes large[11]. However, in assigning  $1/\beta \sim m_\pi$  the tadpole zero mode counts not as  $1/\beta L^3 m_\pi^2$  but rather as  $1/L^3 m_\pi$ . This difference determines a boundary within the  $\epsilon'$  regime above which the counting of  $1/\beta \sim m_\pi$  for a zero mode diagram is legitimate, and below which it is not. This line does not demarcate the boundary between  $\epsilon$  and  $\epsilon'$ , but it does determine the regions where  $1/\beta \sim m_\pi$  counting is appropriate.

#### IV. EVALUATION OF THE ZERO MODES FOR THE $\epsilon$ REGIME

For the  $\epsilon$  regime, the zero modes,  $q_\mu = (0, \vec{0})$ , must be treated nonperturbatively due to the  $1/m_\pi^2 V$  dependence of the pion zero mode propagator. Starting with a purely mesonic theory the Euclidean partition function has the form

$$Z = \int [\mathcal{D}\Sigma] \exp \left[ - \int d^4x \mathcal{L}(\Sigma(x)) \right]. \quad (14)$$

The group element  $\Sigma(x)$  parameterizes the meson fields. The zero and non-zero modes are described by the Fourier components of the pion fields,  $q_n^a$ , in finite volume:

$$\Sigma(x) = \exp\left(\frac{2iM(x) \cdot \tau}{f}\right), \quad M^a(x) = \sum_n q_n^a u_n(x), \quad (15)$$

where  $n$  is a four-vector with integer entries,  $\tau^a$  is one-half the Pauli matrices  $\sigma^a$ , and the  $u_n(x)$ 's are plane waves. Following the procedure of ref. [3], a change of variables is made such that the zero modes are separated from the non-zero modes:

$$\Sigma \rightarrow U \hat{\Sigma} U, \quad (16)$$

$$U = \exp\left(\frac{i\phi \cdot \tau}{f}\right), \quad (17)$$

$$\hat{\Sigma}(x) = \exp\left(\frac{2i\hat{M}(x) \cdot \tau}{f}\right), \quad (18)$$

$$\hat{M}^a(x) = \sum_{n_\mu \neq 0} p_{n_\mu}^a u_{n_\mu}(x). \quad (19)$$

The  $U$ 's are spacetime independent SU(2) matrices containing the zero mode contributions while  $\hat{\Sigma}(x)$  contains the non-zero modes with new Fourier coefficients  $p_n^a$ . Note the  $p_n^a$ 's are related non-linearly to the  $q_n^a$ 's. Using the Baker-Campbell-Hausdorff formula, all the exponentials in eqn (16) can be combined. The resulting exponential has the form:

$$\begin{aligned} U \hat{\Sigma} U &= \exp\left(\frac{2i}{f} \phi^a \tau^a + \frac{2i}{f} \hat{M}^b(x) \tau^b + \frac{1}{2f^2} [2i\phi^a \tau^a, 2i\hat{M}^b(x) \tau^b] + \dots\right) \\ &= \exp\left(\frac{2i}{f} \phi^a \tau^a + \frac{2i}{f} \sum_{n \neq 0} p_n^b u_n(x) \tau^b + \frac{1}{2f^2} \sum_{n \neq 0} u_n(x) [2i\phi^a \tau^a, 2ip_n^b \tau^b] + \dots\right) \end{aligned} \quad (20)$$

where the ellipsis represents an infinite string of commutators involving the  $\phi$  and  $\hat{M}$  matrix. The commutators will always contain at least one power of  $\hat{M}$  making them  $\mathcal{O}(\epsilon)$  or higher. Each of these matrices can in turn be written as sums of their Fourier coefficients multiplied by their appropriate plane wave functions as done above. Since plane waves possess the property that  $u_{n_1}(x)u_{n_2}(x)\dots u_{n_m}(x) = u_{n_1+n_2+\dots+n_m}(x)$  one can expand all the sums and gather all those terms which are multiplied by  $u_{n_1+n_2+\dots+n_m}(x) = u_{n_k}(x)$  for specific  $n_1, n_2, \dots$  and redefine whatever function of the  $p_n^a$ 's and  $\phi^a$ 's that correspond to it, as  $q_{n_k}^a$  for  $n_k \neq 0$ .

When explicitly constructing the measure of integration for the pions,  $[D\Sigma]$ , it includes determinant of the metric of the manifold the fields are defined on. After performing the field redefinition, this factor can be expanded in powers of the non-zero modes of the pion fields[3]:

$$[D\Sigma] = [DU^2] [D\hat{\Sigma}] \sqrt{\det(g)} = [DU^2] [D\hat{\Sigma}] (1 + \mathcal{O}(\hat{\pi}^2)) \quad (21)$$

where  $g$  is the metric. For our calculations only the leading order piece from the metric is needed. When including nucleons the  $\xi(x)$  field is used to describe the mesons in addition to  $\Sigma(x)$ , such that  $\xi^2 = \Sigma$ . Under SU(2) left and

right transformations,  $\Sigma \rightarrow L\Sigma R^\dagger \implies \xi \rightarrow L\xi V^\dagger$  or  $\xi \rightarrow V\xi R^\dagger$  while the nucleons transform according to  $N \rightarrow VN$  such that  $V$  is an  $SU(2)$  matrix that is a function of  $L, R, \xi$ , and  $x$ . Under  $SU(2)$  vector transformations,  $V$  reduces to a spacetime independent element of  $SU(2)_V$  to ensure the correct transformation property of the nucleons.  $V$  is defined implicitly through the following relations:

$$V = \sqrt{L\Sigma R^\dagger} R \xi^\dagger \quad (22)$$

$$V^\dagger = \xi^\dagger L^\dagger \sqrt{L\Sigma R^\dagger} \quad (23)$$

In building chirally invariant terms for the Lagrangian one must use both transformation rules as stated above. It is for this reason that the change of variables needed to separate the zero modes from  $\xi$  are given by the following:

$$\xi \rightarrow U\hat{\xi}V^\dagger \quad (24)$$

$$\xi \rightarrow V\hat{\xi}U \quad (25)$$

and therefore  $V^\dagger = \hat{\xi}^\dagger U^\dagger \sqrt{U\hat{\Sigma}U}$  and  $V = \sqrt{U\hat{\Sigma}U} U^\dagger \hat{\xi}^\dagger$  where  $L = R^\dagger = U$ .

In order to compute the square root of a matrix, assume that there exists a matrix  $D$  such that  $D^2 = U\hat{\Sigma}U$ . Since the non-zero modes are suppressed by a power of  $\epsilon$ , the form of  $D$  is:

$$D = U + \frac{i\epsilon}{f}A - \frac{\epsilon^2}{2f^2}B + \dots \quad (26)$$

where the factors of  $\epsilon$  are made explicit, factors of  $i/f$  were put in for later convenience, and  $A$  and  $B$  can in general depend on the  $p_n^a$ 's and  $\phi^a$ . One can expand  $U\hat{\Sigma}U$  order by order in  $\epsilon$  and set up a matrix equation to determine  $A$  and  $B$ :

$$D^2 = U^2 + \frac{i\epsilon}{f}(UA + AU) - \frac{\epsilon^2}{2f^2}(UB + BU + 2A^2) + \dots \quad (27)$$

$$U\hat{\Sigma}U = U^2 + \frac{2i\epsilon}{f}U\hat{M}^a\tau^aU - \frac{2\epsilon^2}{f^2}U(\hat{M}^a\tau^a)^2U + \dots \quad (28)$$

Hence, one is able to construct  $D$  to the desired order and  $V$  can be readily obtained. Using this to calculate  $V$  one obtains

$$V = \mathbf{1} + \frac{i\epsilon}{f}(-\hat{M} + AU^\dagger) - \frac{\epsilon^2}{2f^2}(\hat{M}^2 - 2AU^\dagger\hat{M} + BU^\dagger) + \mathcal{O}(\epsilon^3) \quad (29)$$

$$\hat{M} = \begin{pmatrix} \hat{\pi}^0/\sqrt{2} & \hat{\pi}^+ \\ \hat{\pi}^- & -\hat{\pi}^0/\sqrt{2} \end{pmatrix} \quad (30)$$

In general  $A$  and  $B$  are complicated functions of the parameters of  $U$  and  $\hat{M}$ . The form of the matrix  $A$  is provided in appendix D, while the matrix  $B$  is not necessary for the calculation at the order considered.

Under the field redefinition using eqns. (16, 24, 25) a few terms in the Lagrangian will be examined to see how they are altered. For the pion-nucleon coupling term given by  $g_A^{(0)}N^\dagger S_\mu \mathcal{A}^\mu N$ , the redefinition causes  $\mathcal{A}_\mu \rightarrow V\hat{\mathcal{A}}_\mu V^\dagger$ , and so expanding the first couple of terms:

$$g_A^{(0)}N^\dagger S_\mu \mathcal{A}^\mu N \rightarrow g_A^{(0)}N^\dagger S_\mu \left( -\frac{2i}{f}\partial^\mu \hat{M} + \frac{2}{f^2} \left\{ [\partial^\mu \hat{M}, \hat{M}] + AU^\dagger \partial^\mu \hat{M} - \partial^\mu \hat{M} U A^\dagger \right\} + \mathcal{O}(\epsilon^3) \right) N \quad (31)$$



It is alarming that  $\mathcal{A}_\mu$  now appears to contain terms which are even in the non-zero mode pion fields since this would violate parity. Generically denoting a zero mode pion field as  $\pi^z$ , then by comparing the  $U$  matrix in the form of:

$$U = \exp \frac{i}{f} \begin{pmatrix} \pi_0^z/\sqrt{2} & \pi_+^z \\ \pi_-^z & -\pi_0^z/\sqrt{2} \end{pmatrix} \quad (32)$$

with that when it is parameterized using hyperspherical coordinates<sup>1</sup>:

$$U = \mathbf{1}\cos(\psi) + i\sigma_1\sin(\psi)\sin(\theta)\cos(\phi) + i\sigma_2\sin(\psi)\sin(\theta)\sin(\phi) + i\sigma_3\sin(\psi)\cos(\theta) \quad (33)$$

leads to the relations:

$$\begin{aligned} \pi_0^z &= \sqrt{2}\psi \cos(\theta) \\ \pi_+^z &= \psi \sin(\theta) \exp(-i\phi) \\ \pi_-^z &= \psi \sin(\theta) \exp(i\phi). \end{aligned}$$

Substituting eqns. (33, 30) in eqn. (31), Taylor expanding the functional dependence in  $\psi$ , and then using the relationships above yield terms with an odd number of non-zero and zero mode pions multiplied by powers of  $\psi^2$ . Because  $\psi^2 = \frac{1}{2}(\pi_0^z)^2 + \pi_+^z\pi_-^z$ , this term will always be even under parity. Hence, the entire contribution is therefore explicitly even under parity. This has been checked to  $\mathcal{O}(1/f^3)$  and will hold for all orders in  $1/f$ .

The relationship between what are called the non-zero modes under the field redefinition ( $\Sigma \rightarrow U\hat{\Sigma}U$ ) versus the non-zero modes in  $\Sigma$  must also be carefully explained. For clarity, an expansion of  $\mathcal{A}_\mu$  to three pion fields with exactly one nonzero mode pion will be considered. In the expansion of the pion-nucleon lagrangian term in eqn. (31) the  $\mathcal{O}(\epsilon)$  term seems to be devoid of zero mode information. Indeed, from the arguments just given, it is reasonable to assume that there should exist some function of the zero modes which accompanies it. However, if we again use the Baker-Campbell-Hausdorff formula to relate the original parametrization to the one in terms of the field redefinition one finds that (where  $\hat{M}'$  encapsulates the non-zero modes before the change of variables and  $\phi$  encapsulates the zero modes):

$$\hat{M} = \hat{M}' + \frac{1}{6f^2} \left[ \phi, \left[ \phi, \hat{M}' \right] \right] + \dots \quad (34)$$

where  $\hat{M}$  is defined by  $\hat{\Sigma} = \exp(2i\hat{M}/f)$ . The definition of  $\hat{M}$  will contain an infinite number of commutators, all of which will be suppressed by a factor of  $\epsilon$  or more. With this definition one can find

$$\begin{aligned} \mathcal{A}_\mu &= \frac{1}{f} \partial_\mu \hat{M} + \mathcal{O}(\hat{M}^2) \\ &\rightarrow \frac{1}{f} \partial_\mu \left( \hat{M}' + \frac{1}{6f^2} \left[ \phi, \left[ \phi, \hat{M}' \right] \right] \right) + \dots \\ &= \frac{1}{f} \partial_\mu \hat{M}' + \frac{1}{6f^3} \left( \phi^2 \partial_\mu \hat{M}' - 2\phi \partial_\mu \hat{M}' \phi + \partial_\mu \hat{M}' \phi^2 \right) + \dots \end{aligned} \quad (35)$$

---

<sup>1</sup> A precise definition of the coordinates used can be found in appendix C. Normally there is a radial coordinate which we denote by  $|b|$  that must exist to parameterize in terms of hyperspherical coordinates. However as shown in the appendix, this factor will be sent to one by the presence of a delta function so we explicitly do not write it for this reason.

This result is identical to the expansion of  $\mathcal{A}_\mu$  prior to making the change of variables. In making the change of variables all that happened was that some of the zero mode information was absorbed into the definition of  $\hat{M}$ . Therefore it is more appropriate to view  $\hat{M}$  not as strictly the non-zero modes of the pions but as an  $\mathcal{O}(\epsilon)$  suppressed quantity with which one can utilize perturbation theory.

For the mass term of the pions, the quark masses will be taken to be equal, hence the change for the mass term is:

$$\begin{aligned} \lambda \frac{f^2}{2} V m_q \text{Tr}(\xi^2 + (\xi^\dagger)^2) &\rightarrow \lambda \frac{f^2}{2} V m_q \text{Tr}(U^2 \hat{\xi}^2 + (U^\dagger)^2 (\hat{\xi}^\dagger)^2) \\ &\simeq \lambda \frac{f^2}{2} V m_q \text{Tr}(U^2 + (U^\dagger)^2) + \mathcal{O}(\epsilon^2). \end{aligned} \quad (36)$$

The first term on the RHS of eqn. (36) counts as an order one term and cannot be expanded. It will therefore have the interpretation of a probabilistic weight function when considering group integrals over  $U^2$ .

Keeping only those terms of the axial-vector current which will contribute to the order at which we work, under the redefinition, it goes to:

$$j_{5\mu}^a = g_A^{(0)} \bar{N} S_\mu V (U \tau^a U^\dagger + U^\dagger \tau^a U) V^\dagger N. \quad (37)$$

One other equivalent method of separating the zero modes circumvents the use of the  $V$  matrix entirely. With this method one simply determines the form of  $\xi = \sqrt{U \hat{\Sigma} U}$  using the same method outlined above and uses this directly in the Lagrangian. It has not been utilized in this paper because the redefinition in terms of the  $V$ 's allows one to immediately write down how terms in the Lagrangian are shifted under the change of variables since it mimics a chiral transformation.

In applying the method described above for integrating over the zero mode portion of the pion fields, care must be taken in the use of the  $V$  and  $V^\dagger$  matrices. Specifically, one must be sure that the expansion in powers of  $\hat{M}$  has been taken far enough to include all of the appropriate zero modes in the calculation. A good example of this is the calculation of the nucleon mass in the  $\epsilon$  regime performed in ref. [10]. To order  $\epsilon^4$  the graphs that contribute to the nucleon mass are given in fig. (3). In fig. 3(a), 3(b), 3(e), and 3(f), the pion couplings are due to one pion derivative interactions from the  $g_A^{(0)}$  and  $g_{\Delta N}$  Lagrangian terms, so to produce these graphs one needs only  $V = \mathbf{1}$ .

The contribution from fig. (3(d)) arises from the terms in the higher order Lagrangian in eqn. (5) proportional to  $\mathcal{A}_0^2$  and  $\mathcal{A}_\mu \mathcal{A}^\mu$ . Under the change of variables these become  $\mathcal{A}_\mu \mathcal{A}^\mu \rightarrow V \hat{\mathcal{A}}_\mu \hat{\mathcal{A}}^\mu V^\dagger \sim V (\partial^\mu \hat{\pi} \partial_\mu \hat{\pi}) V^\dagger$ , where again only  $V = \mathbf{1}$  is required. Finally at this order in  $\epsilon$  is fig. (3(c)), which stems from the Lagrangian term

$$\begin{aligned} \lambda C_1 \bar{N} \text{Tr}[m_q \Sigma^\dagger + h.c.] N &\rightarrow \lambda C_1 \bar{N} \text{Tr}[m_q U^\dagger \hat{\Sigma}^\dagger U^\dagger + h.c.] N \\ &= \lambda C_1 \bar{N} \text{Tr}[m_q (U^\dagger)^2 + h.c.] N + \dots \end{aligned} \quad (38)$$

which explicitly carries zero mode information. This term is evaluated in the same manner as the correction to the

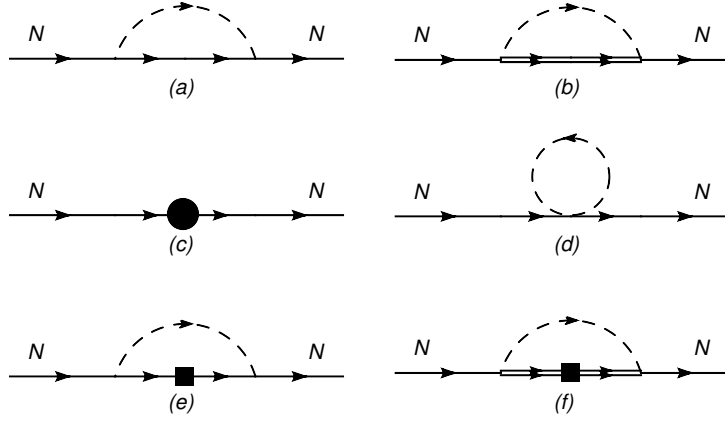


FIG. 3: Graphs that contribute to the nucleon mass up to order  $\epsilon^4$ . The square vertex is an insertion of the kinetic energy operator while the circle is the direct zero mode mass contribution.

pion mass and results in[10]

$$m_B \rightarrow m_B - 4m_\pi^2 C_1 \frac{X'(s)}{2X(s)}$$

$$X(s) = \frac{I_1(2s)}{s} \quad (39)$$

where  $s = \frac{1}{2}m_\pi^2 f^2 V$  and the  $I_n(s)$ 's are modified Bessel functions. The pion mass also has a shifted value due to zero-mode contributions such that  $m_\pi^2 \rightarrow m_\pi^2(s)$ [10], where  $m_\pi^2(s) = m_\pi^2 X'(s)/2X(s)$ . Therefore all  $m_\pi^2$ 's appearing in the computation of the matrix element must be replaced by  $m_\pi^2(s)$ . All of these results are identical to those in ref. [10].

To order  $\epsilon^4$  the method presented above coincides with that of ref. [10] and gives the same result. However, if one wished to carry out the calculation beyond  $\mathcal{O}(\epsilon^4)$  important differences will surface. An inspection of the original Lagrangian will lead to graphs with multiple zero mode loops emanating from the  $\pi NN$  vertex and similar vertices. Fig. (4) displays an example of a graph that will contribute at  $\mathcal{O}(\epsilon^5)$  to the nucleon mass (only one zero mode loop is drawn, though an arbitrary number may exist as they will all be of the same order). In ref. [10] some of this information does not exist. While correct to the order they worked, the field redefinition used in ref. [10] will be incorrect beyond  $\mathcal{O}(\epsilon^4)$ . The inconsistency resides in the field redefinitions according to what is called  $\xi_L$  and  $\xi_R$ . The labels of  $L$  and  $R$  are not to be taken literally, but rather are a device to recall the two different ways  $\xi$  can transform in order to build chirally invariant Lagrangian terms. What is true is that there is only one field, namely  $\xi$ , such that  $\xi^2 = \Sigma$ . This must hold true both before and after the field redefinitions. Initially, the  $\Sigma$  field can be thought of as a generic point on the  $SU(2)$  manifold that is a finite distance away from the identity. Defining  $\xi^2 = \Sigma$  implies that  $\xi$  is located on the midway point of the geodesic connecting  $\Sigma$  to the identity. In the approach of ref. [10], the field redefinitions of  $\xi_L \rightarrow U \hat{\xi}_L$  and  $\xi_R \rightarrow U^\dagger \hat{\xi}_R$  lose this interpretation. The only way to sensibly interpret the meaning of  $\sqrt{U \hat{\Sigma} U}$  is to appeal to the expansion given in eqn. (26). The redefinitions in terms of the  $L$ 's and  $R$ 's does not coincide with this expansion.

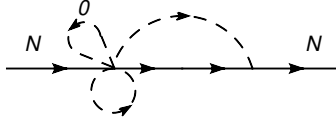


FIG. 4: One graph that contributes to the nucleon mass at order  $\epsilon^5$ . An arbitrary number of zero mode loops can exist at the  $\bar{N}(\hat{\pi}^3)N$  vertex.

Turning to the evaluation of the matrix element of the axial-vector current, the part of the action containing the sources is expanded keeping only the linear term in each. The matrix element to be evaluated is then of the form:

$$\langle N_c(p) | j_{\mu 5}^a | N_b(p) \rangle = \frac{1}{\mathcal{Z}_0} \int [\mathcal{D}\Sigma][\mathcal{D}N] N_b^\dagger(p) j_{\mu 5}^a(q) N_c(p) e^{-\int d^4x \mathcal{L}} \quad (40)$$

where  $\mathcal{Z}_0$  is the partition function free of sources and  $b$  and  $c$  denote particular choices of nucleons from  $N^T = (p, n)$  in the initial and final states.

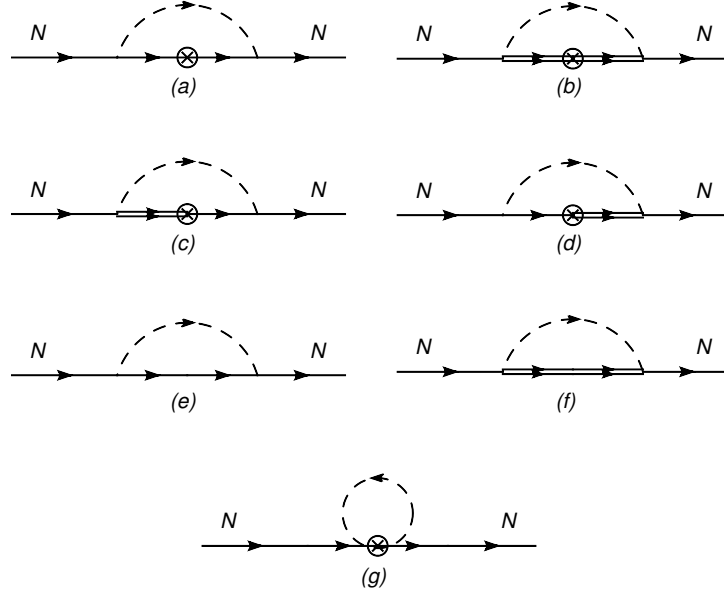


FIG. 5: Graphs that contribute at  $\mathcal{O}(\epsilon^2)$  and  $\mathcal{O}(\epsilon'^2)$ .

The graphs in fig. (5) represent the perturbative contribution to the matrix element and each of these graphs has a function of the zero modes that accompany it which must be integrated over. As an example of how to integrate over the zero modes, consider the tree level contribution:

$$\langle N_c(p) | j_{\mu 5}^a | N_b(p) \rangle_{tree} = g_A^{(0)} (2\bar{N} S_\mu N) (\tau^a)_{mn} \frac{\int [\mathcal{D}U^2] U_{bm}(U^\dagger)_{nc} \exp(s \text{ReTr}(U^2))}{\int [\mathcal{D}U^2] \exp(s \text{ReTr}(U^2))} \quad (41)$$

$$= g_A^{(0)} Q(s) (2\bar{N} S_\mu N) \quad (42)$$

where  $Q(s) = \frac{1}{3} \left( 1 + 2 \frac{I_2(2s)}{I_1(2s)} \right)$ . Here, the  $N$ 's and  $\bar{N}$  are the spinors satisfying  $\frac{1}{2} (1 + v^\mu \gamma_\mu) N = N$  (with a similar relationship for  $\bar{N}$ ) not to be confused with the nucleon field. In the  $s \rightarrow \infty$  limit one recovers the expected answer at tree-level,  $g_A^{(0)}$ .

A contribution which enters at  $\mathcal{O}(\epsilon^2)$  is the one-loop contribution from the axial-vector current as shown in fig. (5(g)). One can determine the function of  $s$  that will modify the graphs from the zero mode integration. The result is:

$$T(s) = \frac{I_0(2s)}{I_1(2s)} - \frac{1}{s}. \quad (43)$$

The other contributions at this order are all multiplied by  $Q(s)$ . The functions  $Q(s)$  and  $T(s)$  are plotted in fig. (6).

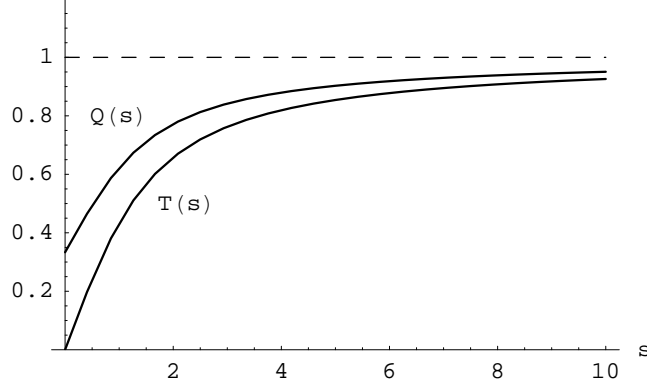


FIG. 6: Zero mode factors  $Q(s)$  and  $T(s)$ .

## V. RESULTS

Putting together all of the contributions from the graphs in figure (5) and using the results from appendix A the result for the  $\epsilon$  regime to  $\mathcal{O}(\epsilon^3)$  is:

$$\begin{aligned} \Gamma_\epsilon(s) = & g_A^{(0)} Q(s) - \frac{Q(s)}{f^2 L^3} \left[ g_A^{(0)} \frac{T(s)}{Q(s)} \frac{c_1 L}{2\pi} + \left( \frac{100}{243} g_{\Delta\Delta} g_{\Delta N}^2 + \frac{4}{3} g_A^{(0)} g_{\Delta N}^2 \right) \left( \frac{c_1 L}{4\pi} - \frac{c_2 \Delta L^2}{4\pi^2} + \frac{c_0}{2m_B} \right) \right. \\ & \left. + \frac{4}{3} (g_A^{(0)})^3 \left( \frac{c_1 L}{4\pi} + \frac{c_0}{2m_B} \right) - \frac{32}{27} g_A^{(0)} g_{\Delta N}^2 \left( \frac{c_1 L}{4\pi} - \frac{c_2 \Delta L^2}{8\pi^2} + \frac{c_0}{2m_B} \right) \right]. \quad (44) \end{aligned}$$

In achieving this result it has been demonstrated in appendix A that the finite time direction corrections in the  $\epsilon$  regime do not enter until  $\mathcal{O}(\epsilon^6)$ , thus significantly reducing the computational burden when working in the  $\epsilon$  regime to orders lower than this.

The result for the  $\epsilon'$  regime utilizes the graphs from fig. (5) as well as from fig. (7). The graphs in fig. (5) are adapted to the  $\epsilon'$  regime by letting  $s \rightarrow \infty$ , which gives  $Q(s) \rightarrow 1$  and  $T(s) \rightarrow 1$ , and adding back the diagrams with

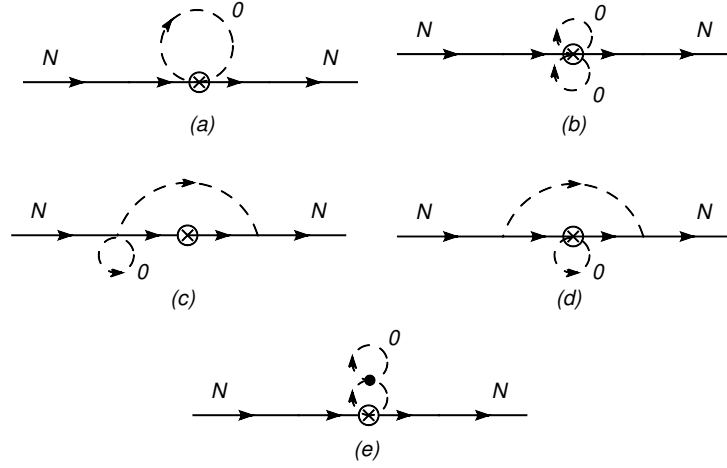


FIG. 7: Additional  $\epsilon'$  graph contributions. Figure (a) enters at  $\mathcal{O}(\epsilon')$ . Figure (b) at  $\mathcal{O}(\epsilon'^2)$ . Figures (c)-(e) are representative of the ways that a zero mode loop can be added to the graphs in fig. 5, in order to create  $\mathcal{O}(\epsilon'^3)$  contributions.

spatial zero modes:

$$\begin{aligned}
\Gamma_{\epsilon'} &= \Gamma_{\epsilon}(s = \infty) + \Gamma_1 + \Gamma_2 + \Gamma_3 \\
\Gamma_1 &= -\frac{g_A^{(0)}}{f^2} \frac{1}{m_\pi L^3} \\
\Gamma_2 &= \frac{g_A^{(0)}}{4f^4} \frac{1}{m_\pi^2 L^6} \\
\Gamma_3 &= \frac{1}{2f^4} \frac{1}{m_\pi L^6} \left[ -\frac{g_A^{(0)}}{20} \frac{1}{m_\pi^2 L^3} + g_A^{(0)} \frac{c_1 L}{4\pi} - \frac{320}{81} g_A^{(0)} g_{\Delta N}^2 \left( \frac{c_1 L}{4\pi} - \frac{c_2 \Delta L^2}{8\pi^2} + \frac{c_0}{2m_B} \right) \right. \\
&\quad \left. + \frac{40}{9} (g_A^{(0)})^3 \left( \frac{c_1 L}{4\pi} + \frac{c_0}{2m_B} \right) + \left( \frac{1000}{729} g_{\Delta N}^2 g_{\Delta\Delta} + \frac{40}{9} g_{\Delta N}^2 g_A^{(0)} \right) \left( \frac{c_1 L}{4\pi} - \frac{c_2 \Delta L^2}{4\pi^2} + \frac{c_0}{2m_B} \right) \right] \\
&\quad + \frac{8}{3} \frac{1}{f^4} \frac{1}{m_\pi L^6} \left( g_A^{(0)} \frac{c_1 L}{4\pi} + (g_A^{(0)})^3 \left( \frac{c_1 L}{4\pi} + \frac{c_0}{2m_B} \right) \right) \\
&\quad + \left( \frac{10}{27} g_{\Delta\Delta} g_{\Delta N}^2 + \frac{10}{9} g_A^{(0)} g_{\Delta N}^2 \right) \left( \frac{c_1 L}{4\pi} - \frac{c_2 \Delta L^2}{4\pi^2} + \frac{c_0}{2m_B} \right) \\
&\quad - \frac{8}{9} g_A^{(0)} g_{\Delta N}^2 \left( \frac{c_1 L}{4\pi} - \frac{c_2 \Delta L^2}{8\pi^2} + \frac{c_0}{2m_B} \right) \Big) \tag{45}
\end{aligned}$$

where the subscripts refer to the order in  $\epsilon'$  considered. In both the  $\epsilon$  and  $\epsilon'$  results given above expansions in  $m_\pi L/2\pi$  and  $\Delta L/2\pi$  have been taken as these quantities count as order  $\epsilon$  and  $\epsilon'$  respectively.

## VI. DISCUSSION AND CONCLUSIONS

In this paper we have discussed the various calculational regimes that are relevant to current lattice calculations. In fig. (2) the approximate extent of these regimes have been demonstrated for different volumes and pion masses, as calculated using the tadpole diagram as a guide. However, it was stressed that these outlines are not to be interpreted as strict boundaries, but rather as midpoints in the smooth transition between the different regimes. From the figure it is clear that as one moves toward a more hypercubical lattice (with the temporal direction the same length as the

spatial extent of the volume) at smaller volumes and more physical pion masses that the  $\epsilon$  and  $\epsilon'$  regimes will be the most important.

Ultimately one would like to use the results from the  $\epsilon$  and  $\epsilon'$  regime in eqns. (44) and (45) to fit to lattice data for  $g_A$  and extrapolate to the physical pion mass value. The majority of the data that exists on lattice calculations of  $g_A$  can be found in refs. [14, 15, 16, 17, 18, 19]. Most of these calculations of the axial current have been performed in the  $\epsilon'$ ,  $\delta$ , or  $p$  regimes according to the separation given above. While there is a significant amount of data available from these calculations, in order to avoid working in the  $\delta$  regime as defined above, only results from volumes significantly greater than  $(2 \text{ fm})^3$  should be used. However, the number of points that strictly satisfy this condition, as well as the condition from eqn. (12) that  $m_\pi L/2\pi < 1$ , is too few for any reasonable fit to be performed.

In ref. [14] a fit to the LHPC Collaboration lattice data was performed using a  $p$  regime calculation of  $g_A$ , as most of these points fall within that regime. The most effective way to efficiently reduce the statistical error in the extrapolation of  $g_A$  at the physical point (where one wishes to compare to experiment) is to perform lattice calculations at lower pion mass ( $< 350 \text{ MeV}$ ). Generally speaking, one low mass calculation may easily be equivalent to three or four high mass calculations in terms of ability to reduce the statistical error of the extrapolation. While performing lower pion mass lattice calculations is often computationally expensive, increases in the speed and number of computers available will soon put these low mass calculations within reach. In addition, a high pion mass moves one further away from the regime of ChPT, adding to statistical considerations concerns about the applicability of the effective field theory, regardless of the regime one is working in. Clearly, the way forward involves lattice calculations at lower pion mass, where the  $\epsilon$  and  $\epsilon'$  regimes will become increasingly important. Our results allow coherent analysis of such data.

In the  $\epsilon$  regime the technique of collective variables was used to separate the spacetime independent zero modes from the spacetime dependent non-zero modes. Before the split into zero and non-zero modes, one is able to see that in graphs where non-zero modes are connected to external states one can have arbitrary numbers of zero mode loops present. These contributions are not lost in the field redefinition. To usefully separate out the order one components of a given contribution it was demonstrated that one must perform the change of variables that is defined by  $\Sigma = U\hat{\Sigma}U$  as in eqn. (16). To correctly include baryon interactions after this change of variables the  $\xi$  objects must be treated carefully with the change of variables given in eqns. (24) and (25). We have described a method for doing this that differs from previous methods[10].

One feature of the method proposed for dealing with the  $\mathcal{O}(1)$  contributions of the pion fields is that the integration over the zero modes must be performed on a diagram by diagram basis. It may seem legitimate to integrate out the zero mode contributions and return a Lagrangian where the relevant coupling constants have been replaced by the appropriate functions of  $s$ , that have been calculated "a posteriori," and with all insertions of the pion fields containing purely non-zero mode information. Doing this, however, would be incorrect. Evaluating higher order diagrams will lead to different zero mode functions multiplying their respective non-zero mode Feynman diagrams. An example of

such a diagram is given in fig. (8). These zero mode functions, in general, will not be encoded in a coupling constant redefinition; it would be misleading to label  $g_A$  as  $g_A(s)$ . As a result, one cannot write down a local Lagrangian after the zero modes have been integrated out. To perform the actual integrations on low order diagrams with relatively simple zero mode contributions one can either use hyperspherical coordinates or use the symmetry properties of the SU(2) group to obtain an answer. However, with more difficult and complicated higher order diagrams hyperspherical coordinates are the most effective tool, as shown in appendix C.

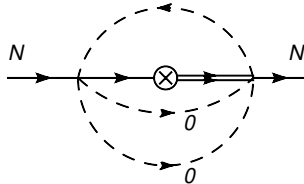


FIG. 8: A diagram for which an integration over the zero modes does not correspond to a simple redefinition of coupling constants.

To conclude, the matrix element of the nucleon axial-vector current has been calculated within the  $\epsilon$  and  $\epsilon'$  regimes to  $\mathcal{O}(\epsilon^3)$  and  $\mathcal{O}(\epsilon'^3)$  respectively. The  $\epsilon'$  regime result agrees to NLO with previous calculations[11]. A method was put forward to calculate the nonperturbative contributions of pion zero momentum modes in the  $\epsilon$  regime in the presence of baryons. This method can be used in any calculation, diagram by diagram, at all orders in the  $\epsilon$  expansion, and was found to differ significantly from previously published procedures[10]. In calculating  $g_A$  it was discovered that the temporal direction could be approximated as infinite, with the errors introduced entering only at the  $\mathcal{O}(\epsilon^6)$  level, as shown in appendix A. This significantly reduces the computational burden of calculations in the  $\epsilon$  regime.

### Acknowledgments

We are very grateful to W. Detmold and M. Savage for their time and many useful conversations. In addition, B.S. and J.W. are indebted to A. Iqbal, D. B. Kaplan, S. Sharpe, M. Endres, C. Kozcaz, C. Spitzer, and A. Walker-Loud for comments and discussions.

## APPENDIX

### APPENDIX A: INTEGRAL & SUM MANIPULATIONS

The integrals used in the calculation of the results in Euclidean space are:

$$R(m_\pi) = \mu^{d-4} \int \frac{d^d q}{(2\pi)^d} \frac{1}{q_0^2 + q^2 + m_\pi^2} \quad (\text{A-1})$$

$$J(\Delta, m_\pi, \beta, L, m_B) = \mu^{d-4} \int \frac{d^d q}{(2\pi)^d} \frac{|\vec{q}|^2}{(iq_0 - \Delta + \vec{q}^2/2m_B)^2} \frac{1}{q^2 + m_\pi^2} \quad (\text{A-2})$$



$$N(\Delta, m_\pi, \beta, L, m_B) = \mu^{d-4} \int \frac{d^d q}{(2\pi)^d} \frac{1}{q^2 + m_\pi^2} \frac{1}{iq_0 - \Delta + \vec{q}^2/(2m_B)} \frac{|\vec{q}|^2}{iq_0 + \vec{q}^2/(2m_B)} \quad (\text{A-3})$$

In the  $\epsilon'$  regime one normally integrates over the  $q_0$  component and forms a sum over the remaining finite volume spatial components, while for the  $\epsilon$  regime a sum over all four components would be formed. However, the  $\epsilon'$  regime can be recovered as a limit of the  $\epsilon$  finite volume manipulations and so one can focus on those.

The sums that arise during our calculation are defined within a dimensional regularization framework so that these should merge smoothly with the infinite volume pieces as  $L \rightarrow \infty$ . Toward this end the sums must be defined by the relation

$$\frac{1}{L^3} \sum_{\vec{q}} = \frac{1}{L^3} \sum_{\vec{q}}^{\Lambda} - \int^{\Lambda} \frac{d^3 q}{(2\pi)^3} + \mu^{d-4} \int^{\text{DR}} \frac{d^{d-1} q}{(2\pi)^{d-1}} \quad (\text{A-4})$$

where the cutoff dependence of the sum is removed by that of the integral. With this definition, the dimensionally regularized integrals will be the infinite volume pieces of the diagram while the remaining sums are the finite volume corrections. The DR pieces will all be proportional to  $m_\pi^2$  or  $\Delta^2$  and so will technically enter at order  $\epsilon^4$  or  $\epsilon'^4$ . However, in order to smoothly merge with the infinite volume result these higher order terms must be included along with a  $\mu$  dependent counterterm. These DR pieces are calculated in the normal way[12].

For the temporal sums found in the  $\epsilon$  regime, the Abel-Plana formula is needed and is given as:

$$\frac{1}{\beta} \sum_n f\left(\frac{2\pi n}{\beta}\right) = \int_{-\infty}^{\infty} \frac{dz}{2\pi} f(z) - i \text{Res} \left( \frac{f(z)}{e^{i\beta z} - 1} \right) \Big|_{\text{lowerplane}} + i \text{Res} \left( \frac{f(z)}{e^{-i\beta z} - 1} \right) \Big|_{\text{upperplane}} \quad (\text{A-5})$$

which is valid if  $f(z)$  has no poles on the real axis. The first term on the right hand side is the infinite time direction piece used in  $\epsilon'$  calculations. One can thus look at eqn. (A-5) as the infinite time  $\epsilon'$  piece plus finite time  $\epsilon$  corrections.

Using eqn. (A-5) the integral from eqn. (A-1) becomes:

$$\begin{aligned} R(m_\pi) &= \int \frac{d^4 q}{(2\pi)^4} \frac{1}{q_0^2 + \vec{q}^2 + m_\pi^2} \\ &= \frac{1}{\beta L^3} \sum_{n_\mu} \frac{1}{(2\pi n_0/\beta)^2 + (2\pi \vec{n}/L)^2 + m_\pi^2} \\ &= \frac{1}{L^3} \sum_{\vec{n}} \left( \frac{1}{\beta} \sum_{n_0} \frac{1}{(2\pi n_0/\beta)^2 + (2\pi \vec{n}/L)^2 + m_\pi^2} \right) \end{aligned} \quad (\text{A-6})$$

Now let  $\beta = aL$  for some value of  $a$  where one expects  $1 \leq a \leq \infty$ . It is now possible to expand the above expression in powers of  $m_\pi L$  as  $m_\pi L \sim \epsilon^\alpha$  with  $\alpha \geq 1$ . Splitting off the zero mode part of this expression and expanding in  $m_\pi L$  gives

$$\begin{aligned} R_0(m_\pi, \beta, L) &= \frac{1}{2} \frac{1}{m_\pi L^3} \\ R_\emptyset(m_\pi, \beta, L) &= \frac{1}{L^3} \sum_{\vec{n} \neq \vec{0}} \frac{L}{4\pi |\vec{n}|} + \frac{1}{L^3} \sum_{\vec{n} \neq \vec{0}} \left( \frac{L}{2\pi |\vec{n}|} \frac{1}{e^{2\pi a |\vec{n}|} - 1} \right) + \mathcal{O}(\epsilon^4) \end{aligned}$$

where the infinite time direction term is the first term on the right and the finite time correction is the second term. Looking at the sums present in each term, the finite time correction will converge very quickly due to the presence of

the exponential. In fact, even for just the first term in the sum the finite time piece will be suppressed by a factor of 267 under the most favorable conditions ( $a = 1$ ). Given that current lattice calculations return  $\epsilon > 1/4$ , the sum for the finite time corrections of the one pion loop is effectively at  $\epsilon^4$  or higher, and so for the  $\epsilon^2$  single pion loop, the finite time corrections are effectively at  $\epsilon^6$  and can be safely ignored. Thus:

$$R_0(m_\pi, \beta, L) = \frac{1}{2} \frac{1}{m_\pi L^3} \quad (\text{A-7})$$

$$R_\emptyset(m_\pi, \beta, L) = \frac{1}{L^3} \sum_{\vec{n} \neq \vec{0}} \frac{L}{4\pi} \frac{1}{|\vec{n}|} + \mathcal{O}(\epsilon^4) \quad (\text{A-8})$$

for both the  $\epsilon$  and  $\epsilon'$  regimes.

For eqns. (A-2) and (A-3) the same procedure is used that was used on eqn. (A-1) with the only modifications being that: (1) the spatial zero modes vanish due to the integrand's proportionality to  $|\vec{q}|^2$ , and (2) the presence of the baryon mass in eqn. (10) must be used in computing the finite volume residues. The residue in the lower half plane and will give a finite time correction of

$$-i\text{Res} \left( \frac{f(z)}{e^{i\beta z} - 1} \right) \Big|_{\text{lower}} \propto \frac{1}{e^{\beta(\Delta+m_B)} - 1} \approx 0 \quad (\text{A-9})$$

as  $m_B \sim \Lambda_\chi$ [10]. The nucleon sector will give the same result with  $\Delta \rightarrow 0$ . Because of this fact which arose due to the finite volume boundary conditions on the relativistic field from eqn. (10), the finite time corrections due to the nucleon and decuplet poles do not contribute. From the above results, the finite time corrections from the pion propagator poles do not contribute at the order we work. Therefore, to order  $\mathcal{O}(\epsilon^3)$ , the finite time contributions to the sums are negligible and only the infinite time direction contributions are needed.

Calculating eqn. (A-2) explicitly and expanding in  $m_\pi L$  and  $\Delta L$ :

$$\begin{aligned} J(\Delta, m_\pi, \beta, L, m_B) &= \frac{1}{\beta L^3} \sum_{n_\mu} \frac{(2\pi\vec{n}/L)^2}{(i(2\pi n_0/\beta) - \Delta + (2\pi\vec{n}/L)^2/2m_B)^2} \frac{1}{(2\pi n_0/\beta)^2 + (2\pi\vec{n}/L)^2 + m_\pi^2} \\ &= \frac{1}{L^3} \sum_{\vec{n} \neq \vec{0}} \left( \frac{L}{4\pi} \frac{1}{|\vec{n}|} - \frac{\Delta L^2}{4\pi^2} \frac{1}{|\vec{n}|^2} + \frac{1}{2m_B} \right) + \mathcal{O}(\epsilon^4) \end{aligned} \quad (\text{A-10})$$

For eqn. (A-3) it is easier to generalize the integral:

$$N'(A, B, m_\pi, \beta, L, m_B) = \int \frac{d^4 q}{(2\pi)^4} \frac{1}{q^2 + m_\pi^2} \frac{1}{iq_0 - A + q^2/(2m_B)} \frac{|\vec{q}|^2}{iq_0 - B + q^2/(2m_B)} \quad (\text{A-11})$$

$$N(\Delta, m_\pi, \beta, L, m_B) = N'(\Delta, 0, m_\pi, \beta, L, m_B) \quad (\text{A-12})$$

Using similar methods to those used to evaluate the function  $J$  and taking  $A \rightarrow \Delta$  and  $B \rightarrow 0$  gives

$$N(\Delta, m_\pi, \beta, L, m_B) = \frac{1}{L^3} \sum_{\vec{n} \neq \vec{0}} \left( \frac{L}{4\pi} \frac{1}{|\vec{n}|} - \frac{\Delta L^2}{8\pi^2} \frac{1}{|\vec{n}|^2} + \frac{1}{2m_B} \right) + \mathcal{O}(\epsilon^4) \quad (\text{A-13})$$

For each of the resulting equations one is left with a spatial sum over various powers of  $|\vec{n}|$ . Several of these sums contain divergent pieces which must be removed and placed in appropriate counterterms. Defining these sums as the

limit of an analytically continued sum from non-integer powers of  $|\vec{n}|$ , one can indeed obtain the finite pieces that are necessary. This results in[25, 26]:

$$\begin{aligned} c_2 &= \sum_{\vec{n} \neq 0} \frac{1}{|\vec{n}|^2} = -8.913633 \\ c_1 &= \sum_{\vec{n} \neq 0} \frac{1}{|\vec{n}|} = -2.8372974 \\ c_0 &= \sum_{\vec{n} \neq 0} 1 = -1 \end{aligned} \tag{A-14}$$

With these coefficients the sums above become

$$R_0(m_\pi, \beta, L) = \frac{1}{2} \frac{1}{m_\pi L^3} \tag{A-15}$$

$$R_\emptyset(m_\pi, \beta, L) = \frac{1}{L^3} \frac{c_1 L}{4\pi} + \mathcal{O}(\epsilon^4) \tag{A-16}$$

$$J(\Delta, m_\pi, \beta, L, m_B) = \frac{1}{L^3} \left( \frac{c_1 L}{4\pi} - \frac{c_2 \Delta L^2}{4\pi^2} + \frac{c_0}{2m_B} \right) + \mathcal{O}(\epsilon^4) \tag{A-17}$$

$$N(\Delta, m_\pi, \beta, L, m_B) = \frac{1}{L^3} \left( \frac{c_1 L}{4\pi} - \frac{c_2 \Delta L^2}{8\pi^2} + \frac{c_0}{2m_B} \right) + \mathcal{O}(\epsilon^4) \tag{A-18}$$

## APPENDIX B: CONTRIBUTING DIAGRAMS

### 1. Order $\epsilon'$ Graphs

For the graph in fig. 7(a) the zero next to the pion loop indicates that we are only interested in the zero momentum mode of this pion loop. This graph contributes to  $\mathcal{O}(\epsilon')$ . Its contribution is

$$\Gamma_1 = -\frac{2g_A^{(0)}}{f^2} R_0(m_\pi, \beta, L) \bar{N} S^\mu N \tag{B-1}$$

### 2. Order $\epsilon^2$ and $\epsilon'^2$ Graphs

The graphs in fig. 5(a)-(d) yield[11]:

$$\Gamma_{2a} = \frac{1}{6f^2} (g_A^{(0)})^3 Q(s) J(0, m_\pi, \beta, L, m_B) \bar{N} S^\mu N \tag{B-2}$$

$$\Gamma_{2b} = -\frac{100}{243} \frac{g_{\Delta\Delta} g_{\Delta N}^2 Q(s)}{f^2} J(\Delta, m_\pi, \beta, L, m_B) \bar{N} S^\mu N \tag{B-3}$$

$$\Gamma_{2c} = \Gamma_{2d} = \frac{32}{27} \frac{g_A^{(0)} g_{\Delta N}^2 Q(s)}{f^2} N(\Delta, m_\pi, \beta, L, m_B) \bar{N} S^\mu N \tag{B-4}$$

The two graphs which contribute to field renormalization are given in figs. 5(e) and (f).

$$\Gamma_{2e} = -\frac{3}{2} \frac{(g_A^{(0)})^3 Q(s)}{f^2} J(0, m_\pi, \beta, L, m_B) \bar{N} S^\mu N \tag{B-5}$$

$$\Gamma_{2f} = -\frac{4}{3} \frac{g_A^{(0)} g_{\Delta N}^2 Q(s)}{f^2} J(\Delta, m_\pi, \beta, L, m_B) \bar{N} S^\mu N \tag{B-6}$$

Figure 5(g) gives:

$$-\frac{2g_A^{(0)}T(s)}{f^2}R_\emptyset(m_\pi, \beta, L)\bar{N}S^\mu N \quad (\text{B-7})$$

and fig. 7(b) give a contribution of:

$$\frac{g_A^{(0)}}{f^4}[R_\emptyset(m_\pi, \beta, L)]^2\bar{N}S^\mu N \quad (\text{B-8})$$

where the function  $R_\emptyset(m_\pi, \beta, L)$  is the non-zero mode portion of the function  $R(m_\pi)$ .

### 3. Order $\epsilon^3$ and $\epsilon'^3$ Graphs

At order  $\epsilon'^3$ , there exist contributions from graphs such as those shown in fig. 7(c) and (d). To generate these graphs one adds a spatial zero mode loop to each vertex in fig. 5(a). As these contain spatial zero mode pion loops they contribute only to  $\mathcal{O}(\epsilon'^3)$  and not to  $\mathcal{O}(\epsilon^3)$ . Adding a zero mode pion loop to the  $\mathcal{O}(\epsilon^2)$  graphs at every vertex on every graph, including the field renormalization graphs, will generate the majority of the  $\mathcal{O}(\epsilon'^3)$  contributions. The effect of adding these pion zero mode loops will be to change the coefficient due to that vertex and multiply the previous expressions by the pion loop integral  $R_0(m_\pi)$ . None of the Clebsch-Gordan coefficients or the spin operator contractions will change from those used at  $\mathcal{O}(\epsilon'^2)$ . To find the change to the vertex coefficients one needs to look at each vertex in turn.

By carefully expanding the vertex terms in the Lagrangian to three pions one can derive the change that occurs to the graphs found when a zero mode pion loop is added to figs. (5(a)-(f)). Upon completing the expansion to three pions, such a change simply multiplies the graphs from  $\mathcal{O}(\epsilon'^2)$  by a factor of  $-\frac{2}{3f^2}R_0(m_\pi, \beta, L)$ . In addition, one can add such a zero mode loop to either end of the graph so that there are two distinct configurations. Hence, adding a zero mode pion loop to the Lagrangian vertex will give an  $\mathcal{O}(\epsilon'^3)$  contribution that looks like

$$\begin{aligned} \Gamma_{3a} = & \left( -\frac{4}{3f^2}R_0(m_\pi, \beta, L) \right) \left( -\frac{1}{f^2} \left[ \frac{100}{243}g_{\Delta N}^2g_{\Delta\Delta}J(\Delta, m_\pi, \beta, L, m_B) \right. \right. \\ & + \frac{4}{3}g_A^{(0)}g_{\Delta N}^2J(\Delta, m_\pi, \beta, L, m_B) + \frac{4}{3}(g_A^{(0)})^3J(0, m_\pi, \beta, L, m_B) \\ & \left. \left. - \frac{32}{27}g_A^{(0)}g_{\Delta N}^2N(\Delta, m_\pi, \beta, L, m_B) \right] \right) \bar{N}S^\mu N \quad (\text{B-9}) \end{aligned}$$

$\mathcal{O}(\epsilon'^3)$  diagrams are also produced by adding a zero mode pion loop to the vertex due to the current for each of the graphs in fig. (5) as well as the contribution from fig. 7(b). This includes adding a zero mode loop to the current vertex that is implicitly part of the field renormalization graphs, creating an  $\mathcal{O}(\epsilon'^3)$  contribution that effectively combines the contribution from fig. 7(a) with the field renormalizations of figs. 5(e) and (f). Figures 5(a)-(f) are multiplied by a factor of  $-\frac{2}{f^2}R_0(m_\pi, \beta, L)$ , while fig. 5(g) is multiplied by  $-\frac{1}{2f^2}R_0(m_\pi, \beta, L)$ , fig. 7(b) is multiplied

by  $-\frac{1}{5f^2}R_0(m_\pi, \beta, L)$ . Putting all of these current insertion loops together yields a contribution of

$$\begin{aligned} \Gamma_{3b} = & \left( -\frac{1}{5}\frac{g_A^{(0)}}{f^6}[R_0(m_\pi, \beta, L)]^3 + \frac{g_A^{(0)}}{f^4}R_0(m_\pi, \beta, L)R_\emptyset(m_\pi, \beta, L) \right. \\ & - \frac{2}{f^2}R_0(m_\pi, \beta, L) \left( -\frac{1}{f^2} \left[ \frac{100}{243}g_{\Delta N}^2 g_{\Delta\Delta} J(\Delta, m_\pi, \beta, L, m_B) \right. \right. \\ & + \frac{4}{3}g_A^{(0)}g_{\Delta N}^2 J(\Delta, m_\pi, \beta, L, m_B) + \frac{4}{3}(g_A^{(0)})^3 J(0, m_\pi, \beta, L, m_B) \\ & \left. \left. - \frac{32}{27}g_A^{(0)}g_{\Delta N}^2 N(\Delta, m_\pi, \beta, L, m_B) \right] \right) \bar{N}S^\mu N \end{aligned} \quad (\text{B-10})$$

The final  $\mathcal{O}(\epsilon'^3)$  graphs are those as in fig. 7(e), where the vertex denoted by the dot is from an expansion of the pion kinetic energy term. This will generate a four pion vertex, and by choosing the correct contractions of the pion fields a zero mode loop can be added as shown to each of the graphs in fig. (5). This gives a contribution of

$$\begin{aligned} \Gamma_{3c} = & \frac{32}{3}\frac{g_A^{(0)}}{f^4}R_\emptyset(m_\pi, \beta, L)\frac{d}{dm_\pi^2}R_0(m_\pi, \beta, L) + \frac{16}{3f^4}R_0(m_\pi, \beta, L) \left( 2g_A^{(0)} \left[ R_\emptyset(m_\pi, \beta, L) + m_\pi^2 \frac{d}{dm_\pi^2}R_\emptyset(m_\pi, \beta, L) \right] \right. \\ & + (g_A^{(0)})^3 \left[ J(0, m_\pi, \beta, L, m_B) + m_\pi^2 \frac{d}{dm_\pi^2}J(0, m_\pi, \beta, L, m_B) \right] \\ & + \left( \frac{10}{27}g_{\Delta\Delta}g_{\Delta N}^2 + \frac{10}{9}g_A^{(0)}g_{\Delta N}^2 \right) \left[ J(\Delta, m_\pi, \beta, L, m_B) + m_\pi^2 \frac{d}{dm_\pi^2}J(\Delta, m_\pi, \beta, L, m_B) \right] \\ & \left. - \frac{8}{9}g_A^{(0)}g_{\Delta N}^2 \left[ N(\Delta, m_\pi, \beta, L, m_B) + m_\pi^2 \frac{d}{dm_\pi^2}N(\Delta, m_\pi, \beta, L, m_B) \right] \right) \bar{N}S^\mu N \end{aligned} \quad (\text{B-11})$$

From an operator point of view, both the  $\epsilon$  and  $\epsilon'$  regimes have graphs of  $\mathcal{O}(\epsilon^3)$  and  $\mathcal{O}(\epsilon'^3)$  that look like that in fig. (9). The square vertex is an insertion of the operator from the  $\mathcal{O}(1/m_B)$  Lagrangian terms found in eqn. (5). However, these graphs have been automatically accounted for by the choice of propagator when the  $\mathcal{O}(1/m_B)$  terms were included.

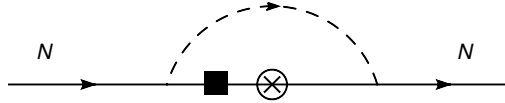


FIG. 9: Example of operator insertions from the  $\mathcal{O}(1/m_B)$  Lagrangian. This graph would contribute at  $\mathcal{O}(\epsilon'^3)$  and  $\mathcal{O}(\epsilon^3)$  but is already counted by the choice of propagator.

### APPENDIX C: HAAR MEASURE

The integration measure to be used for the zero mode is  $[DU^2]$  (parameterized with hyperspherical coordinates):

$$\int [DU^2] = \frac{1}{\pi^2} \int d^4a \delta(a^2 - 1) \quad (\text{C-1})$$

such that  $U^2 = a_0\mathbf{1} + i\vec{a} \cdot \vec{\sigma}$  and the integral is normalized to one. For the calculations in this paper  $U = b_0\mathbf{1} + i\vec{b} \cdot \vec{\sigma}$  is parameterized in terms of hyperspherical coordinates:  $|b| \in [0, \infty]$ ,  $\psi \in [0, \pi]$ ,  $\theta \in [0, \pi]$ , and  $\phi \in [0, 2\pi]$  giving

$$U = |b|\cos(\psi)\mathbf{1} + i|b|\sin(\psi)\sin(\theta)\cos(\phi)\sigma_1 + i|b|\sin(\psi)\sin(\theta)\sin(\phi)\sigma_2 + i|b|\sin(\psi)\cos(\theta)\sigma_3 \quad (\text{C-2})$$

In order to express the integration measure in terms of the radial and angular coordinates describing  $U$  we merely have to calculate a Jacobian factor. The result obtained is:

$$\begin{aligned} \int [\mathcal{D}U^2] &\rightarrow \frac{1}{4\pi^2} \int d^4b (16b^4 \cos^2(\psi)) \delta(b^2 - 1) \\ &= \frac{4}{\pi^2} \int db b^7 \delta(b^2 - 1) \int d\psi d\theta d\phi \sin^2(\psi) \cos^2(\psi) \sin(\theta) \end{aligned} \quad (\text{C-3})$$

where in the first line the prefactor of  $1/4$  is present so the integral is properly normalized and the parenthetical factor is the Jacobian.

The integral in the numerator of eqn. (41) can be done by parameterizing the zero mode variable,  $U$ , in terms of hyperspherical coordinates or in this particular example it can be done directly. To see this, the integrand and measure in eqn. (41) must be invariant under multiplication on the left and right by arbitrary constant  $SU(2)$  matrices. This implies that the integral must have the form:

$$\int [\mathcal{D}U^2] U_{bm}(U^\dagger)_{nc} \exp(s \text{ReTr}(U^2)) = A(s) \delta_{bc} \delta_{mn} + B(s) \delta_{bm} \delta_{nc} \quad (\text{C-4})$$

Contracting indices and using the relation  $\int [\mathcal{D}U^2] \exp(s \text{ReTr}(U^2)) = X(s)$  [3, 27], and  $2 \det U = (\text{Tr } U)^2 - \text{Tr } U^2$  (valid for  $SU(2)$  matrices) one will obtain:

$$A(s) = \frac{1}{6} (2X(s) - X'(s)) \quad (\text{C-5})$$

$$B(s) = \frac{1}{3} (X(s) + X'(s)) \quad (\text{C-6})$$

## APPENDIX D: MATRIX DEFINITIONS

The form of the matrix  $A$  defined earlier in the paper has the following structure (using the hyperspherical parametrization from eqn. (33)):

$$\begin{aligned}
A_{11} = & \frac{1}{\sqrt{2}}\hat{\pi}_0\cos(\psi) + \frac{i}{\sqrt{2}}\hat{\pi}_0\cos(\theta)\sin(\psi) + \frac{i}{2}e^{-i\phi}\hat{\pi}_-\sin(\theta)\sin(\psi) + \frac{i}{2}e^{-i\phi}\hat{\pi}_+\sin(\theta)\sin(\psi) \\
& - \frac{i}{2}e^{-i\phi}\hat{\pi}_-\cos(\theta)\sin(\theta)\sin(\psi)\tan(\psi) - \frac{i}{2}e^{-i\phi}\hat{\pi}_+\cos(\theta)\sin(\theta)\sin(\psi)\tan(\psi) \\
& + \frac{1}{\sqrt{2}}\hat{\pi}_0\sin^2(\theta)\sin(\psi)\tan(\psi)
\end{aligned} \tag{D-1}$$

$$\begin{aligned}
A_{12} = & \hat{\pi}_+\cos(\psi) - \frac{1}{4}e^{-2i\phi}\hat{\pi}_-\sin(\psi)\tan(\psi) + \frac{3}{4}\hat{\pi}_+\sin(\psi)\tan(\psi) + \frac{1}{4}e^{-2i\phi}\hat{\pi}_-\cos(2\theta)\sin(\psi)\tan(\psi) \\
& + \frac{1}{4}\hat{\pi}_+\cos(2\theta)\sin(\psi)\tan(\psi) - \frac{1}{2\sqrt{2}}e^{-i\phi}\hat{\pi}_0\sin(2\theta)\sin(\psi)\tan(\psi)
\end{aligned} \tag{D-2}$$

$$\begin{aligned}
A_{21} = & \hat{\pi}_-\cos(\psi) + \hat{\pi}_-\cos^2(\theta)\sin(\psi)\tan(\psi) - \frac{1}{\sqrt{2}}e^{i\phi}\hat{\pi}_0\cos(\theta)\sin(\theta)\sin(\psi)\tan(\psi) \\
& + \frac{1}{2}\hat{\pi}_-\sin^2(\theta)\sin(\psi)\tan(\psi) - \frac{1}{2}e^{2i\phi}\hat{\pi}_+\sin^2(\theta)\sin(\psi)\tan(\psi)
\end{aligned} \tag{D-3}$$

$$\begin{aligned}
A_{22} = & -\frac{1}{\sqrt{2}}\hat{\pi}_0\cos(\psi) + \frac{i}{\sqrt{2}}\hat{\pi}_0\cos(\theta)\sin(\psi) + \frac{i}{2}e^{-i\phi}\hat{\pi}_-\sin(\theta)\sin(\psi) + \frac{i}{2}e^{i\phi}\hat{\pi}_+\sin(\theta)\sin(\psi) \\
& + \frac{i}{2}e^{-i\phi}\hat{\pi}_-\cos(\theta)\sin(\theta)\sin(\psi)\tan(\psi) + \frac{i}{2}e^{i\phi}\hat{\pi}_+\cos(\theta)\sin(\theta)\sin(\psi)\tan(\psi) \\
& - \frac{1}{\sqrt{2}}\hat{\pi}_0\sin^2(\theta)\sin(\psi)\tan(\psi)
\end{aligned} \tag{D-4}$$

- 
- [1] E. Jenkins and A. V. Manohar (1991), talk presented at the Workshop on Effective Field Theories of the Standard Model, Dobogoko, Hungary, Aug 1991.
- [2] M. Luscher, Commun. Math. Phys. **104**, 177 (1986).
- [3] J. Gasser and H. Leutwyler, Phys. Lett. **B188**, 477 (1987).
- [4] F. C. Hansen, Nucl. Phys. **B345**, 685 (1990).
- [5] F. C. Hansen and H. Leutwyler, Nucl. Phys. **B350**, 201 (1991).
- [6] F. C. Hansen (1990), bUTP-90-42-BERN.
- [7] P. Hasenfratz and H. Leutwyler, Nucl. Phys. **B343**, 241 (1990).
- [8] A. Hasenfratz et al., Z. Phys. **C46**, 257 (1990).
- [9] H. Leutwyler and A. Smilga, Phys. Rev. **D46**, 5607 (1992).
- [10] P. F. Bedaque, H. W. Griesshammer, and G. Rupak, Phys. Rev. **D71**, 054015 (2005), hep-lat/0407009.
- [11] W. Detmold and M. J. Savage, Phys. Lett. **B599**, 32 (2004), hep-lat/0407008.
- [12] S. R. Beane and M. J. Savage, Phys. Rev. **D70**, 074029 (2004), hep-ph/0404131.
- [13] E. Jenkins and A. V. Manohar, Phys. Lett. **B259**, 353 (1991).
- [14] R. G. Edwards et al. (LHPC), Phys. Rev. Lett. **96**, 052001 (2006), hep-lat/0510062.
- [15] D. Dolgov et al. (LHPC), Phys. Rev. **D66**, 034506 (2002), hep-lat/0201021.
- [16] S. Ohta and K. Orginos (RBCK), Nucl. Phys. Proc. Suppl. **140**, 396 (2005), hep-lat/0411008.
- [17] A. A. Khan et al., Nucl. Phys. Proc. Suppl. **140**, 408 (2005), hep-lat/0409161.
- [18] A. A. Khan et al., Phys. Rev. **D74**, 094508 (2006), hep-lat/0603028.
- [19] S. Capitani et al., Nucl. Phys. Proc. Suppl. **79**, 548 (1999), hep-ph/9905573.
- [20] E. Jenkins and A. V. Manohar, Phys. Lett. **B255**, 558 (1991).
- [21] M. E. Luke and A. V. Manohar, Phys. Lett. **B286**, 348 (1992), hep-ph/9205228.
- [22] A. F. Falk, B. Grinstein, and M. E. Luke, Nucl. Phys. **B357**, 185 (1991).
- [23] A. Walker-Loud, Nucl. Phys. **A747**, 476 (2005), hep-lat/0405007.
- [24] H. Leutwyler, Phys. Lett. **B189**, 197 (1987).
- [25] A. Edery, J. Phys. **A39**, 685 (2006), math-ph/0510056.
- [26] M. Luscher, Commun. Math. Phys. **105**, 153 (1986).
- [27] M. Creutz (1983), Cambridge, UK: Univ. Pr. (1983) 169 P. (Cambridge Monographs On Mathematical Physics).